ADIABATIC FORMULATION AND ORGANIZATION OF ECMWF'S SPECTRAL MODEL

BY

A.P.M. BAEDE *), M. JARRAUD AND U. CUBASCH

*) Present address:
KNMI (Royal Netherlands Meteorological Institute)
Postbus 201
3730 AE De Bilt
The Netherlands

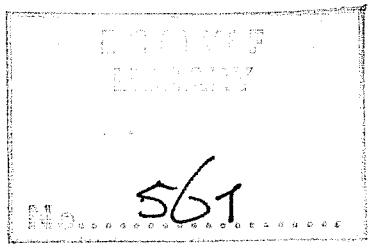

CONTENTS PAGE NUMBER

Summary

The formulation and organization of ECMWF's adiabatic spectral model are discussed. The formulation is conventional and rather similar to that of the models of Bourke (1974) and Hoskins and Simmons (1975). The organization of the model is tuned to minimum core storage requirements and maximum efficiency and flexibility, although it is realised that the last two conditions may sometimes be conflicting. Core storage is minimized by adopting a double gaussian loop structure and allowing I/O of grid point data. High efficiency, in particular on vector machines, is obtained by a diagonal-wise storage of spectral coefficients. This system also allows high flexibility with respect to the choice of the truncation and the integration domain.

On ECMWF's CRAY-1 computer (0.75 Mwords) integrations are possible within the order of 5000 spectral degrees of freedom.

CHAPTER I

Introduction

The spectral modelling technique has been developed over the last few years to a mature stage. Some weather services make use already of operational spectral models, and development of such models is in progress at several other institutes. A comprehensive review of the mathematical aspects is given by Machenhauer (1978). A description of operational spectral models is found in papers by Bourke et al. (1977) and Daley et al. (1976).

Although the spectral technique has proven to be efficient and accurate, its major draw-back has been its high core storage demand. This prohibited the development of the very high resolution models that may be necessary for successful extended range weather forecasting. The solution of this problem is therefore of paramount importance for the development of ECMWF's spectral model.

In this report we describe both the formulation and the organization carried out at ECMWF. The formulation is described in Chapter II with details given in two appendices. The organization is presented in Chapter III. Particular attention has been paid to the problem of vectorization of the code in order to increase the efficiency on ECMWF's Cray-1 computer system. Integrations on this system are possible in the T60-80 range with 15 vertical levels.

Table 1 Constants and variables used in the model

t	time
λ	longitude
$\mu = \sin \theta$	sine of latitude
ζ	absolute vorticity
D	divergence
u	longitudinal velocity component
v	latitudinal velocity component
$U = u.\sqrt{1-\mu^2}$	u cos θ
$V = v\sqrt{1-\mu^2}$	v cos θ
q	humidity mixing ratio
T	temperature
T_o	reference temperature, constant in time and only dependent on σ.
$T' = T-T_o$	
$T_v = T \frac{0.622+q}{0.622(1+q)}$	virtual temperature
$T_v' = T_v-T_o$	
p_*	surface pressure
p	pressure
$\sigma = \frac{p}{p_*}$	vertical coordinate
$\dot{\sigma} = \frac{d\sigma}{dt}$	sigma vertical velocity
$\omega = \frac{dp}{dt}$	pressure vertical velocity
ϕ	geopotential
ϕ_*	geopotential of earth's surface
a	radius of earth
R	gas constant
C_p	specific heat at constant pressure
$\kappa = R/C_p$	

CHAPTER II

Formulation of the model

1. The model equations

The continuous equations are similar to those used by Bourke (1974) and Hoskins and Simmons (1976). Instead of the momentum equations the following two equations for vorticity and divergence are used:

$$\frac{\partial \zeta}{\partial t} = \frac{1}{a(1-\mu^2)} \frac{\partial}{\partial \lambda}(F_v+P_v) - \frac{\partial}{a\partial \mu}(F_u+P_u) \qquad (1.1)$$

$$\frac{\partial D}{\partial t} = \frac{1}{a(1-\mu^2)} \frac{\partial}{\partial \lambda}(F_u+P_u) + \frac{\partial}{a\partial \mu}(F_v+P_v) - \nabla^2\left(\frac{U^2+V^2}{2(1-\mu^2)}+\phi+ RT_o \ell n p_*\right) \qquad (1.2)$$

where:

$$F_u = V.\zeta - \dot{\sigma}\frac{\partial U}{\partial \sigma} - R.T'_v \frac{\partial \ell n p_*}{a\partial \lambda}$$

$$F_v = - U.\zeta - \dot{\sigma}\frac{\partial V}{\partial \sigma} - RT'_v (1-\mu^2) \frac{\partial \ell n p_*}{a\partial \mu}$$

$$T'_v(\lambda,\mu,\sigma) = T_v(\lambda,\mu,\sigma) - T_o(\sigma)$$

T_v being the virtual temperature

$$T_v = T. \frac{0.622+q}{0.622(1+q)}$$

and $T_o(\sigma)$ an arbitrary vertical temperature profile.

The non-adiabatic forcing terms P_u and P_v and those in the equations below are not discussed in this report, except for the horizontal diffusion in Section 7. A list of all symbols used in this chapter is presented in Table 1 (page 2).

The thermodynamic equation and the equation for the mixing ratio can be written as follows:

$$\frac{\partial T'}{\partial t} = -\frac{1}{a(1-\mu^2)}\frac{\partial}{\partial \lambda}(U.T') - \frac{\partial}{a\partial \mu}(V.T') + D.T' - \dot{\sigma}\frac{\partial T}{\partial \sigma} + \kappa\frac{T_v \omega}{p} + P_T \qquad (1.3)$$

$$\frac{\partial q}{\partial t} = -\frac{1}{a(1-\mu^2)}\frac{\partial}{\partial \lambda}(U.q) - \frac{\partial}{a\partial \mu}(V.q) + D.q - \dot{\sigma}\frac{\partial q}{\partial \sigma} + P_q \qquad (1.4)$$

Here $T'(\lambda,\mu,\sigma) = T(\lambda,\mu,\sigma) - T_o(\sigma)$

and q is the mixing ratio.

The pressure vertical velocity ω in the thermodynamic equation is defined by

$$\frac{\omega}{p} = \vec{v}.\nabla \ell np_* - \frac{1}{\sigma}\int_o^\sigma (D+\vec{v}.\nabla \ell np_*)d\sigma \qquad (1.5)$$

whereas the sigma vertical velocity $\dot{\sigma}$ is given by

$$\dot{\sigma} = \sigma\int_o^1 (D+\vec{v}.\nabla \ell np_*)d\sigma - \int_o^\sigma (D+\vec{v}.\nabla \ell np_*)d\sigma \qquad (1.6)$$

The reasons for using the flux form rather than the advective form of the temperature and mixing ratio equations will become obvious later in this report (page 20).

From the continuity equation in the σ-system:

$$\frac{\partial \ell np_*}{\partial t} = -\vec{v}.\nabla \ell np_* - \nabla.\vec{v} - \frac{\partial \dot{\sigma}}{\partial \sigma} \qquad (1.7)$$

and using the boundary conditions:

$$\dot{\sigma} = 0 \text{ for } \sigma = 0 \text{ and } \sigma = 1 \qquad (1.8)$$

we easily derive the following prognostic equation for the surface pressure by vertical integration

$$\frac{\partial \ell n p_*}{\partial t} = - \int_0^1 (D + \vec{v}.\nabla \ell n p_*) d\sigma \qquad (1.9)$$

Assuming the atmosphere to be a perfect mixture of dry air and water vapour, the hydrostatic equation can be written as

$$\frac{\partial \phi}{\partial \ell n \sigma} = - R.T_v \qquad (1.10)$$

ϕ being the geopotential and R being the gas constant for dry air.

2. The horizontal spectral representation

All prognostic quantities ζ,D,T,q and $\ell n p_*$ are represented in the horizontal by a truncated series of spherical harmonics

$$X(\lambda,\mu,\sigma,t) = \sum_{m=-M}^{+M} \sum_{n=|m|}^{N(m)} X_{m,n}(\sigma,t).P_{m,n}(\mu).e^{im\lambda}$$

where $X_{m,n}(\sigma,t)$ are the complex spectral coefficients and $P_{m,n}(\mu)$ are Associated Legendre Polynomials. The use of ζ and D as prognostic quantities directly implies a consistent truncation of the velocity components U and V (Bourke, 1974).

Besides the prognostic quantities, also the orography ϕ_* and the geopotential ϕ are represented by the same truncated series.

At present there seems to be no conclusive evidence in favour of any particular choice of the form of the truncation N(m). It was therefore decided to allow for maximum flexibility by adopting a so-called pentagonal truncation,

depicted in Fig. 2.1. This truncation is completely defined by three parameters J, K and M. All common truncations are special cases of the pentagonal one

triangular	$M = J = K$
rhomboidal	$K = J + M$
trapezoidal	$K = J,\ K > M$

Furthermore, the model equations may be integrated optionally on the globe or on the hemisphere by making use of the parity of the prognostic quantities. In order to compute the non-linear terms in the spectral prognostic equations, the transform method (Machenhauer, 1978) is applied. Non-linear terms of any order may be computed exactly within the assumed truncation if the transform grid is defined on a sufficient number of gaussian lines of latitude and equally spaced lines of longitude. It has been shown however, (Hoskins and Simmons (1975)) that in practice it is sufficient to allow for an unaliased computation of only the quadratic terms.

In order to find the necessary number of gaussian lines of latitude for a pentagonal truncation, the product truncation for quadratic terms must be constructed. The general form of this product truncation together with the original truncation is shown in Fig. 2.2 in which quantity N is defined as:

$$N = K - J$$

It should be noted that the triangular indentation in the upper boundary disappears if $M - N \geq 2N$ i.e. if $M \geq 3N$. From this figure and the exactness condition for the gaussian integration it may be shown that the number of gaussian latitudes G must fulfil the following conditions.

$$\text{if } M \leq 2N \qquad G \geq \frac{2J+K+M+1}{2}$$

$$\text{if } M \geq 2N \qquad G \geq \frac{3K+1}{2}$$

These conditions reduce to those for the common truncations:

Triangular/Trapezoidal $N=0 \Rightarrow M \geq 2N \quad G \geq \frac{3K+1}{2}$

Rhomboidal $M=N \leq 2N \quad G \geq \frac{3J+2M+1}{2}$

In order to obtain an exact Fourier integration of quadratic terms on a line of latitude, the number of longitude points P must fulfil the following condition, independent of the type of truncation:

$$P \geq 3M+1$$

3. The vertical finite difference representation

Several methods have been investigated to represent the vertical structure of the prognostic variables. For a brief review of the attempts to introduce Galerkin methods, we refer to the recent paper by Staniforth and Daley (1977). In this model we adopted the more conventional finite difference approach, similar to the formulation of Hoskins and Simmons (1975) and identical to that of ECMWF's grid point model (Burridge and Haseler, 1977).

The vertical distribution of variables is shown in Fig. 3.1. All prognostic quantities are carried on full σ-levels, whereas the vertical velocity $\dot{\sigma}$ is carried on half σ-levels, subject to the boundary conditions (1.8).

Defining

$$\Delta\sigma_k = \sigma_{k+\frac{1}{2}} - \sigma_{k-\frac{1}{2}}$$

the vertical advection terms have the following finite

difference analogue

$$(\dot{\sigma}\,\frac{\partial X}{\partial \sigma})_k \rightarrow \frac{1}{2\Delta\sigma_k}\left[\dot{\sigma}_{k+\frac{1}{2}}(X_{k+1}-X_k) + \dot{\sigma}_{k-\frac{1}{2}}(X_k-X_{k-1})\right]$$

The vertical integrals in the expression (1.6) for $\dot{\sigma}$ and in equation (1.9) are approximated as follows:

$$\dot{\sigma}_{k+\frac{1}{2}} = \sigma_{k+\frac{1}{2}} \cdot \sum_{j=1}^{N} (D_j + \vec{v}_j . \nabla \ell n p_*)\Delta\sigma_j - \sum_{j=1}^{k} (D_j + \vec{v}_j . \nabla \ell n p_*)\Delta\sigma_j$$

$$\frac{\partial\, \ell n p_*}{\partial t} = -\sum_{j=1}^{N} (D_j + \vec{v}_j . \nabla \ell n p_*)\Delta\sigma_j$$

N being the number of levels.

The vertical integral in the conversion term (1.5) is special in that it is intimately connected with the integration of the hydrostatic equation (1.10). This will be discussed in the next section.

4. The integration of the hydrostatic equation

Integration of (1.10) gives the following expression for the height of the k-th level.

$$\phi_k = \phi_* - R \int_{\sigma=1}^{\sigma=\sigma_k} T_v . d\ell n\sigma \qquad (4.1)$$

Consider a finite difference approximation of this equation

$$\phi_k = \phi_* + R \sum_{\ell=k}^{N} B_{k\ell}\, T_{v\ell} \qquad (4.2)$$

where $B_{k\ell}$ are elements of an, as yet unspecified, upper-triangular matrix $\underline{\underline{B}}$. Now, in order to ensure a cancellation of the transformations between kinetic and potential energy, it can be shown that the conversion term (1.5) of the thermodynamic equation must be represented by the following finite difference analogue.

$$(\frac{\kappa T_v \omega}{p})_k = \kappa T_{vk}[\vec{v}_k . \nabla_\ell np_* - \sum_{\ell=1}^{k} C_{k\ell}(D_\ell + v_\ell . \nabla_\ell np_*)]$$

where the elements $C_{k\ell}$ of the lower-triangular matrix $\underline{\underline{C}}$ are related to those of $\underline{\underline{B}}$ by

$$C_{k\ell} = B_{\ell k} \cdot \frac{\Delta\sigma_\ell}{\Delta\sigma_k}$$

This general scheme has been implemented in the spectral model, by leaving it to the user to provide the model with the desired matrix $\underline{\underline{B}}$. The program then computes matrix $\underline{\underline{C}}$ and the scheme is therefore energy conserving for any arbitrary upper triangular integration matrix $\underline{\underline{B}}$. One easily shows that the schemes of Hoskins and Simmons (1975) and Burridge and Haseler (1977) are special cases of this general scheme.

As a default option, the integration of the hydrostatic equation following Burridge and Haseler (1977) has been implemented. In this scheme the integration proceeds from half level to half level:

$$\phi_{k+\frac{1}{2}} = \phi_* + R \sum_{\ell=k+1}^{N} T_{v\ell} \cdot \ell n \frac{\sigma_{\ell+\frac{1}{2}}}{\sigma_{\ell-\frac{1}{2}}}$$

and the values at the full levels are found by simple averaging

$$\phi_k = \tfrac{1}{2}(\phi_{k+\frac{1}{2}} + \phi_{k-\frac{1}{2}})$$

The geopotential of the top level however is found by extrapolation

$$\phi_1 = \phi_{1\frac{1}{2}} + RT_1 \ln \frac{\sigma_{1\frac{1}{2}}}{\sigma_1}$$

This leads to the following values of the elements of matrix $\underline{\underline{B}}$.

$$B_{k\ell} = 0 \qquad \ell < k$$

$$B_{kk} = \tfrac{1}{2} \ln \frac{\sigma_{k+\frac{1}{2}}}{\sigma_{k-\frac{1}{2}}} \qquad k \neq 1$$

$$= \ln \frac{\sigma_{1\frac{1}{2}}}{\sigma_1} \qquad k = 1$$

$$B_{k\ell} = \ln \frac{\sigma_{\ell+\frac{1}{2}}}{\sigma_{\ell-\frac{1}{2}}} \qquad \ell > k$$

Although the vertical scheme ensures mass and energy conservation, these quantities are still not conserved exactly due to time truncation and round-off errors and, in case of energy, due to the horizontal scheme. As was shown, however, by Hoskins and Simmons (1975) and Baede et al. (1976) the spurious change of these quantities is extremely small. In the latter paper it was shown that the non-conservation of mass is dominated by time truncation errors, whereas the spurious change of the total energy can be explained by round-off errors.

It was furthermore pointed out by Hoskins and Simmons (1975) that the vertical scheme presented in this section does not conserve angular momentum, in contrast with Arakawa's (1972) vertical scheme. They were able to show however that the effect of this property on a simulation of a developing baroclinic wave was negligible.

5. The semi-implicit time stepping scheme

Following the approach and notation of Hoskins and Simmons, the prognostic equations (1.1) - (1-9) may be written in the following way after using the vertical scheme introduced in the previous two paragraphs.

$$\frac{\partial \zeta_{\downarrow}}{\partial t} - Z_{\downarrow} = 0 \tag{5.1}$$

$$\frac{\partial D_{\downarrow}}{\partial t} - \mathcal{D}_{\downarrow} = -\nabla^2(\phi_* + R\underline{\underline{B}}T_{\downarrow} + RT_{o\downarrow}\ell np_*) - \nabla^2(R\underline{\underline{B}}(T_{v\downarrow} - T_{\downarrow})) \tag{5.2}$$

$$\frac{\partial T_{\downarrow}}{\partial t} - \mathcal{T}_{\downarrow} = -\underline{\underline{\tau}}.D_{\downarrow} \tag{5.3}$$

$$\frac{\partial \ell np_*}{\partial t} - P = -\vec{\pi}.D_{\downarrow} \tag{5.4}$$

$$\frac{\partial q_{\downarrow}}{\partial t} - \mathcal{Q}_{\downarrow} = 0 \tag{5.5}$$

Here vertical arrows indicate column-vectors and the horizontal arrow a row vector. All terms on the right hand side of the equations are linear gravity wave terms, resulting from a linearization of the atmosphere about the vertical reference temperature profile To(σ). The actual form of the terms $Z, \mathcal{D}, \mathcal{T}, \mathcal{Q}, P$, the matrix $\underline{\underline{\tau}}$ and the row vector $\vec{\pi}$ are not important here. They are all given in appendix 1. Some remarks should be made however concerning the gravity wave term in the thermodynamic equation. In principle it contains all those contributions to the temperature tendency in which the reference temperature To is multiplied by the divergence. Such contributions come from both the vertical advection term and the conversion term. It was however shown by Bourke et al. (1977) that a semi-implicit scheme, based only on

the contributions from the conversion term is stable and might have certain advantages. In the present model, however, all linear terms have been taken into account. A discussion of the stability properties of the semi-implicit scheme as a function of the reference temperature (To(σ)) is given in Simmons et al. (1978).

Now introducing a spectral representation of the prognostic quantities, a leapfrog finite difference analogue of the time derivatives and an implicit treatment of the linear gravity wave terms, we obtain the following set of finite difference prognostic equations:

$$\delta_t \zeta_{m,n\downarrow} = Z_{m,n\downarrow} \tag{5.6}$$

$$\delta_t q_{m,n\downarrow} = Q_{m,n\downarrow} \tag{5.7}$$

$$\delta_t D_{m,n} = \mathcal{D}_{m,n\downarrow} + \frac{n(n+1)}{a^2}\left(\phi_{*m,n} + \underline{\underline{R}}\underline{B}\bar{T}^t_{m,n\downarrow} + RT_{o\downarrow}\overline{\ell np}^t_{*m,n} + \underline{\underline{R}}\underline{B}\tau_{v_{m,n}}\right) \tag{5.8}$$

$$\delta_t T'_{m.n\downarrow} = \mathcal{T}_{m,n} - \underline{\underline{\tau}}.\bar{D}^t_{m,n\downarrow} \tag{5.9}$$

$$\delta_t \ \ell np_{*m,n} = P_{m,n} - \vec{\pi}.\bar{D}^t_{m,n\downarrow} \tag{5.10}$$

where

$$\delta_t X = (X^{t+\Delta t} - X^{t-\Delta t}) \ / \ 2\Delta t$$

and

$$\bar{X}^t = \tfrac{1}{2}(X^{t+\Delta t} + X^{t-\Delta t})$$

Note that since T_v cannot be treated implicitly we write $T_v = T+(T_v-T)$ and we treat $\tau_v = T_v-T$ explicitly.

From equations (5.8-5.10), together with the hydrostatic equation (4.2), the following equation for $\bar{D}^t_{m,n}$ may be derived:

$$\underline{\underline{A}}_n . \bar{D}^t_{m,n\downarrow} = \frac{a^2}{n(n+1)} D^{t-t}_{m,n\downarrow} + \Delta t.\left(\frac{a^2}{n(n+1)} \mathcal{D}_{m,n\downarrow} + R\underline{\underline{B}}^T V_{m,n\downarrow}\right.$$

$$+ \Phi_{*m,n} + R.\underline{\underline{B}}\ T^{t-\Delta t}_{m,n\downarrow} + R\ T_{o\downarrow}.\ell n p^{t-t}_{*m,n} + \Delta t.R.\underline{\underline{B}}^T_{m,n\downarrow}$$

$$\left. + \Delta t.RT_{o\downarrow}.P_{m,n}\right) \qquad (5.11)$$

where the constant matrix $\underline{\underline{A}}n$ is defined by:

$$\underline{\underline{A}}_n = \frac{a^2}{n(n+1)}\ \underline{\underline{I}} + R\Delta T^2(\underline{\underline{B}}\ \underline{\underline{\tau}} + T_{o\downarrow}.\vec{\pi}.)$$

$\underline{\underline{I}}$ being the unit matrix.

Finally we obtain a new prognostic equation for the divergence which follows directly from the definition of $\bar{D}^t$.

$$\delta_t\, D_{m,n\downarrow} = \frac{\bar{D}^t_{m,n\downarrow} - D^{t-\Delta t}_{m,n\downarrow}}{\Delta t} \qquad (5.12)$$

The set of equations (5.6), (5.7), (5.9) - (5.12) forms a complete set of prognostic spectral finite difference equations of the model. However we have added to this model a time smoother for numerical reasons, and horizontal diffusion for numerical and physical reasons. They will be discussed in the next two sections.

6. Time smoothing

It is well known that in order to avoid the growth of the computational mode associated with the leap frog scheme, a linear timefilter might be useful.

$$\bar{X}_t = X_t + \alpha(\bar{X}_{t-\Delta t} - 2X_t + X_{t+\Delta t})$$

where α is a small number, typically in the order of 0.005. Due to the linearity of this filter, it may be applied in grid point space as well as in spectral space. Because, as will be seen later, in spectral space only one time level

of data is available at any time, and in grid point space two time levels, it was decided to apply the filter on all prognostic quantities in grid point space in two steps, each requiring only two time levels.

$$\tilde{X}_t = X_t + \alpha(X_{t-\Delta t} - 2X_t)$$

$$\bar{X}_t = \tilde{X}_t + \alpha X_{t+\Delta t}$$

7. Horizontal diffusion

In order to avoid a spurious growth of amplitudes at wave numbers near the truncation wave number known as spectral blocking, a crude parameterization of the transport processes to the smaller, unresolved, scales may be necessary. This parameterization generally takes the form of a linear or non-linear horizontal diffusion. In view of its easy implementation in spectral models and its high scale selectivity, we choose a linear ∇^4 horizontal diffusion on σ-surfaces. Because, as said before, only one time level of data is available in spectral space, an implicit scheme was implemented according to

$$\frac{X_{t+\Delta t} - X_{t-\Delta t}}{2\Delta t} = \left(\frac{\partial X_t}{\partial t}\right)_{ad} - K.\nabla^4 X_{t+\Delta t}$$

where the first term on the r.h.s. of the equation represents the adiabatic tendency. In spectral form this leads to:

$$X_{m,n}^{t+\Delta t} = \frac{a^4}{a^4+2\Delta t K n^2(n+1)^2}\left[X_{m,n}^{t-\Delta t} + 2\Delta t \left(\frac{\partial X_{m,n}^t}{\partial t}\right)_{ad}\right]$$

It can therefore be considered as a correction to the prognostic variables after completion of the adiabatic timestep.

In order to avoid damping of uniform rotations (n=1) on the sphere the diffusive correction of vorticity and divergence takes the form: (Bourke et al., 1977 and Orszag, 1974)

$$\frac{a^4}{a^4+2\Delta t K\left|n^2(n+1)^2-\bar{4}\right|}$$

being equal to

$$1 \text{ for } n = 1$$

Application of the horizontal diffusion on σ surfaces may lead to spurious diffusion near steep topography. In other models this problem was avoided by performing the diffusion on pressure surfaces followed by interpolation to σ surfaces. But there is no conclusive evidence in favour of such a procedure.

The above implicit diffusion scheme is slightly inconsistent with the semi-implicit time stepping scheme in that the computation of $\bar{D}^t_{m,n}$ and therefore of the linear gravity wave terms is based on the undiffused divergence $D^{t+\Delta t}_{m,n}$. Again, however, in view of the small diffusion coefficient and of the fact that horizontal diffusion is anyhow a rather crude parameterization, this seems not to be a serious problem. Test integrations have shown that it does not lead to any numerical instabilities.

It remains to be shown if horizontal diffusion is necessary at all. This may depend on such factors as the horizontal truncation, the length of the forecasting period and the physical parameterization scheme. For example, the Canadian group (Daley et al. (1976)) was able to produce short range forecasts without horizontal diffusion.

8. Transformation between spectral and grid point space

As stated in section 2 of this chapter, the transform method is used to compute the non-linear quantities in the spectral prognostic equations. This requires transformations back and forth between spectral and grid point space. The algebra involved has been spelled out in several publications (Daley et al. 1976), (Bourke et al., 1977), (Machenhauer, 1978) and needs not be repeated here. An exception is made for the expressions used to compute the velocity components U and V on the gaussian grid. In previously published models it was found necessary to compute first the spectral components $U_{m,n}$ and $V_{m,n}$ within a truncation large enough to yield exactly equivalent spectral representations of $\{U,V\}$ and $\{\zeta,D\}$. This then was followed by a straightforward computation of the grid point values of the velocity components. However, because a spectral representation of U and V is nowhere in the model explicitly required, it was found a considerable advantage to compute the velocity gridpoint values using the following expressions:

$$\{U,V\} = \sum_{m=-M}^{+M} \{U_m,V_m\} e^{im\lambda}$$

with:

$$U_m = -a \sum_{n=|m|}^{N(m)} \left[\frac{im}{n(n+1)} D_{m,n} P_{m,n}(\mu_j) - \frac{1}{n(n+1)} \zeta_{m,n} \cdot (1-\mu_j^2) \frac{dP_{m,n}}{d\mu}(\mu_j) \right] \tag{8.1}$$

$$V_m = -a \sum_{n=|m|}^{N(m)} \left[\frac{im}{n(n+1)} \zeta_{m,n} P_{m,n}(\mu_j) + \frac{1}{n(n+1)} D_{m,n} \cdot (1-\mu_j^2) \frac{dP_{m,n}}{d\mu}(\mu_j) \right] \tag{8.2}$$

Apart from avoiding the storage of spectral velocity components, it has the extra advantage that the same truncation is used throughout the model.

CHAPTER III

Organisation of the Model

9. Constraints

The development of ECMWF's spectral model was subject to several constraints which we shall outline here in rather arbitrary order:

a) Within the core storage constraints of ECMWF's operational computer facilities (about 0.75M word core available to the user), high resolution spectral integrations must be feasible. In a triangular truncation the maximum zonal wave number should be in the range 60-80, with 15-levels in the vertical.

b) The model must be compatible with ECMWF's grid point model with respect to data and history file format and with respect to the implementation of the physical parameterization scheme.

c) If any I/O is necessary to meet the above requirements, it must be possible to mask it with the computational CPU-time.

d) The code must be flexible with respect to the type of truncation and with respect to the integration domain (global or hemispheric).

e) The code must run efficiently on ECMWF's vector machine.

The first constraint was met by elaborating a scheme suggested by Burridge (private communication) that makes it possible to limit the number of fields of spectral

components to one for each prognostic variable and each vertical level. This is achieved at the expense of some I/O of grid point data and some corresponding extra buffers in core. This extra core, however, increases only linearly with resolution whereas the core required for spectral components increases quadratically. This organisation scheme is worked out in detail in section 10.

The fact that there is only I/O of grid point data makes the I/O easy. The I/O, the grid point data and the file structure are identical to those of ECMWF's grid point model. Thus this meets the second requirement.

Whether also the third constraint is met is a point of further investigation and will depend, among others, on the final operational computer configuration.

No serious problems were encountered in the vectorization of the code, except for the legendre transform from spectral space to grid point space. This problem was solved by a diagonalwise arrangement in one-dimensional arrays of the spectral components. This will be elaborated in detail in section 11.

Bearing in mind that all spectral components on a diagonal in the (m,n) plane have the same parity, the proposed arrangement of spectral components makes it very easy to implement flexibility with respect to both the type of truncation and the integration domain. This is discussed in section 12.

The fact that at any time only one time-level of spectral data is available creates some problems with respect to the semi-implicit scheme. The expression in square brackets on the r.h.s. of equation (5.11) cannot be computed in spectral space because two time levels and tendencies are required simultaneously. The formulae used

to compute this term on the gaussian grid are presented in a second appendix.

10. The double loop structure

The traditional approach of the organisation of a spectral model is to perform the computation in one loop per timestep over the gaussian latitudes. The non-local nature of the spectral approach requires that all spectral coefficients should be kept intact during the scan. If, moreover, two time levels of grid point variables are required, it follows that in the traditional approach three complete fields of spectral coefficients per vertical level of each prognostic variable are needed: one for the previous time level, one for the present and one for the tendencies. These core requirements prohibit high resolution integrations unless the use of peripheral I/O devices is permitted. Layer-by-layer I/O of spectral coefficients, however, seems unsuitable because the introduction of physical parameterization schemes is simplified if grid point values are available simultaneously at all levels. This would increase I/O time to a level out of proportion to CPU-time.

An organisation scheme with two transform loops per time step was proposed by Bourke et al. (1977). One loop handles the physical processes, the other one the dynamics. Although some reduction of core storage is claimed it has the disadvantage of extra transforms. An unexplored advantage of this approach may be that different grid resolutions could be used in both loops in order to minimise aliasing due to the highly non-linear physical processes.

To achieve substantially higher resolutions, a further decrease of, in particular, spectral coefficient storage is necessary. The amount of I/O time involved however

should not exceed computational CPU-time so that masking is possible.

The scheme proposed here limits the number of fields of spectral components to one for each prognostic variable and each vertical level, at the expense of I/O of grid point data and some extra grid point buffers in core. The amount and the format of I/O is such that compatibility with the grid point model with respect to data storage can easily be achieved. The principal of the scheme is as follows:
Consider a centred time step:

$$S_{n+1} = S_{n-1} + 2\Delta t \frac{\partial S_n}{\partial t}$$

At the beginning of time step n a field of spectral coefficients S_n is available in core in a buffer SB. In a first gaussian loop the corresponding grid point values G_n are computed and temporarily stored on disk. In the second gaussian loop grid point values G_{n-1} and G_n at time levels n-1 and n are read from disk. Next on each latitude line the contributions to S_{n-1} and $2\Delta t \frac{\partial S_n}{\partial t}$ are computed and their sum accumulated in the same buffer SB. Clearly the advantage is that one spectral field SB is sufficient. The fact that never more than one time level of spectral data is available has, however, some disadvantages which will be discussed below.

Elaboration of this scheme is complicated by the time smoothing, the convective adjustment and the semi-implicit time stepping scheme, but no serious problems were encountered. The complete scheme will now be described in some detail and is presented schematically in fig.10.1.

At the beginning of a timestep n we have available the spectral coefficients of the prognostic variables $\hat{S}_n$, which have not been subject to time smoothing and

convective adjustment. In the first loop the corresponding gaussian grid point values are computed. Whilst computations on row j are in progress, grid point values of row j-1 are written to disk A. At the end of the loop all information is essentially available on disk A and the spectral fields may be blanked. In the second loop these grid point data are read in again from disk A and at the same time half-time-smoothed grid point data $\hat{G}_{n-1}$ are read from disk B. These data were written to this disk in the second loop of the previous time step (see below). Of course data for row j+1 are read with computations on row j progressing simultaneously.

First of all present time step data $\hat{G}_n$ are convectively adjusted. It should be noted that these adjusted data are used in the subsequent computation of adiabatic and non-adiabatic tendencies without re-analysis and truncation in spectral space. This is in contrast with the Australian model (Bourke et al, 1977).

It should be noted furthermore that problems arise if a convective adjustment scheme should be applied that computes vertical momentum exchange. This would result in an inconsistency between the velocity fields on one hand and vorticity and divergence on the other. Here the advantage of the flux form of the temperature and humidity equations becomes clear. Had the advective form been chosen, adjustment of T and q would have made it necessary to recompute the corresponding horizontal space derivatives of these quantities in order to avoid inconsistencies.

After convective adjustment the time smoothing of $\tilde{G}_{n-1}$ can be completed. This means that from now on we dispose of convectively adjusted present time step values G_n and time smoothed values $\bar{G}_{n-1}$ of the previous time step. This is then the best opportunity to produce so-called history files, containing results for verification and display.

Here also the first part of the time filter (equation 6.2) is applied to G_n. The results are produced in a special buffer for output to disk B.

On the basis of G_n and $\bar{G}_{n-1}$ adiabatic and non-adiabatic tendencies may be computed now. As far as possible these tendencies are added to $\bar{G}_{n-1}$ for transformation to spectral space. Those parts of the tendencies which involve horizontal derivatives are kept and transformed separately. Finally, all relevant quantities are transformed to spectral space and the contribution of the current row j to $\bar{S}_{n-1} + 2\Delta t \left(\frac{\partial S_n}{\partial t}\right)$ is added to the spectral field in core.

After completion of the second loop, the timestep is finished except for the linear semi-implicit contribution to the tendencies and for the horizontal diffusion. As mentioned above, the r.h.s. of the Helmholtz equation (5.11) is accumulated in the course of the second loop. After transformation the r.h.s. is stored in a special spectral field, reserved for this purpose. Here finally the Helmholtz equation is solved and the semi-implicit linear contributions are added. The time step is completed by applying horizontal diffusion according to equation (7.2).

Fig.10.2 presents the total core storage required for spectral and gridpoint fields in an adiabatic model, as a function of triangular truncation. The full curve is the sum of spectral and grid point fields, the dashed curve, the grid point fields only. The discontinuities stem from the assumption that the number of grid points on a gaussian latitude line is a power of 2 and fulfils moreover equation (2.2). Clearly, adiabatic integrations up to T80 are feasible on ECMWF's CRAY-1 computer with its 0.75M word core storage. Moreover, sufficient core memory is left for a sophisticated physical parameterization scheme at least up to T70.

In Fig.10.3 the amount of I/O is shown in k-words per time step. Again the step function behaviour stems from the power of 2 assumption and from the fact that the I/O concern grid point data only. The actual I/O time involved is a much more important figure but cannot be given here because it depends on the actual configuration of peripheral storage devices. In particular, in the second loop I/O to and from three different files take place simultaneously. The I/O time to CPU-time ratio may therefore be optimised by storing these files on three different disks, each with its own processor.

Against the advantage of a considerable core storage reduction must be set the disadvantage of having only one time level of spectral data available, as already mentioned above. This makes it necessary to compute the r.h.s. of the Helmholtz equation in grid point space and to perform extra transforms back to spectral space. A further consequence is that the hydrostatic equation is integrated in grid points, rather than in spectral space. This saves again a spectral field in core. Expressions used for the r.h.s. of the Helmholtz equation in grid point space are presented in the last section. First we shall discuss the solution of the vectorization problem.

11. Vectorization of the Legendre transform

For vectorization purposes, the computations in a spectral model may conveniently be classified in five groups:

a) grid point computations, including the physical parameterization schemes;

b) Fast Fourier transforms;

c) contributions from each gaussian latitude to the inverse Legendre transforms to spectral space;

d) spectral computations (e.g. horizontal diffusion; semi-implicit part);

e) Legendre transforms.

Grid point computations are vectorized easily by inner loops over the grid points on a latitude line. A vectorized FFT routine was obtained from C. Temperton, ECMWF, and need not concern us here. Also, the spectral computations and the inverse Legendre transforms are easily vectorized, whatever way of storage of the spectral coefficients is chosen. The traditional column-wise storage of spectral coefficients in one-dimensional arrays (Fig.11.1b) however is unsuitable to the vectorization of the Legendre transforms, where sums of the type:

$$X_m(\mu_j) = \sum_n P_{m,n}(\mu_j) X_{m,n}$$

are computed for each m within the truncation. The problem is that the array index increments n rather than m. Storage in double-indexed arrays offers a solution but seems rather inconvenient in case of any other than rhomboidal truncation.

We choose to store the spectral coefficients diagonal-wise in one-dimensional arrays so that the array index increments both m and n (Fig.11.1a). The inner vector loop is then a loop over all (m,n) points on a diagonal. The length of the diagonal is fixed in an outer loop over all diagonals.

Clearly for low resolution, vectorization may be rather inefficient, particularly in case of triangular truncation where the length of the vector loop is decreasing linearly. For high resolution this problem is less important however. Nevertheless, in a vectorized spectral code efficiency may be an important criterion in selecting a type of truncation.

12. Truncation and integration domain

The diagonal-wise storage of spectral coefficients offers a convenient way of introducing flexibility in the code, both with respect to the choice of the truncation and with respect to the integration domain. This stems from the fact that all coefficients on a diagonal have the same parity. A global model can therefore be transformed easily into a hemispheric one by skipping every second diagonal. This avoids such artificial features as the "jagged" truncation (Hoskins and Simmons, 1975). At the same time flexibility with respect to the choice of the truncation is obtained by specifying in a one-dimensional array the length of each diagonal, the only condition being that all (m,n) points on a diagonal actually belong to the truncation domain. As already explained in section 2, we choose to restrict ourselves to a pentagonal truncation which, by specifying the values of three parameters may be reduced to the common triangular, rhomboidal and trapezoidal truncations.

It is realised that this high flexibility may be at the expense of efficiency, by causing considerable over-head in setting up the vector-loops. The present model should therefore be considered as an experimental model for research purposes. For an operational model, the Legendre transforms should be rewritten for a specific truncation and integration domain, preferably in Assembler Language.

Acknowledgements

We thank Aksel W. Hansen for his contributions in the very early stages of the development of the model. He suggested the flexible vertical scheme described in section 1.4. We are grateful to Dave Burridge for his original suggestion of a double gaussian loop structure and his continuous stimulating interest in the project. Without the support of Tony Hollingsworth the birth of this model would have been much more traumatic. We acknowledge gratefully Eva Edberg's expertise in the development of the code.

References

Arakawa, A. (1972) Design of the UCLA general circulation model, UCLA Met.Dep. Tech. Report No. 7.

Baede, A.P.M., Dent, D. and Hollingsworth, A. (1976) The Effect of Arithmetic Precision on some Meteorological Integrations. ECMWF Technical Report No.2.

Bourke, W. (1974) A multi-level spectral model. I. Formulation and hemispheric integrations. Mon.Weath.Rev., 102, pp. 687-701.

Bourke, W., McAvaney, B., Puri, K. and Thurling, R. (1977) Global modelling of atmospheric flow by spectral methods. Methods in Computational Physics Vol. 17: General Circulation Models of the Atmosphere Ed. J.Chang, Academic Press, pp. 267-324.

Burridge D.M. and Haseler, J. (1977) A model for medium range weather forecasting, adiabatic formulation ECMWF Technical Report No.4.

Daley, R., Girard, C., Henderson, J. and Simmonds, I. (1976) Short term forecasting with a multi-level spectral primitive equations model. Atmosphere, 14, pp.98-134.

Hoskins, B.J. and Simmons, A.J. (1975) A multi-layer spectral model and the semi-implicit method. Quart.J.Roy.Met.Soc., 101, pp. 637-655.

Machenhauer, B. (1978) The Spectral Method Numerical Methods used in Atmospheric Models, Vol. II.

Orszag, S.A. (1974) Fourier Series on Spheres Mon.Weath.Rev. 106, pp. 405-412.

References (contd.)

Simmons, A.J., Hoskins, B.J. and Burridge, D.M. (1978) Stability of the semi-implicit methods of time integration. Mon. Weath. Rev., 106, pp. 405-412.

Staniforth, A.N. and Daley, R. (1977) A finite-element formulation for the vertical discretisation of sigma-coordinate primitive equation models. Mon. Weath. Rev. 105, pp. 1108-1118.

Appendix 1

The non-linear quantities in the prognostic equation (5-1)-(5.5) are defined as follows: (suffix k indicates the vertical level)

$$Z_k = \left[\frac{1}{a(1-\mu^2)} \frac{\partial}{\partial\lambda} F_v - \frac{\partial}{a\partial\mu} F_u\right]_k$$

$$D_k = \left[\frac{1}{a(1-\mu^2)} \frac{\partial}{\partial\lambda} F_u + \frac{\partial}{a\partial\mu} F_v\right]_k - \nabla^2 E_k$$

$$E_k = \frac{U_k^2 + V_k^2}{2(1-\mu^2)}$$

$$T_k = T1_k + T2_k$$

with

$$T1_k = -\frac{1}{a(1-\mu^2)} \frac{\partial}{\partial\lambda} (U_k . T'_k) - \frac{\partial}{a\partial\mu} (V_k T'_k)$$

$$T2_k = D_k T'_k - \frac{1}{2\Delta\sigma_k}\left[\dot{\sigma}_{k+\frac{1}{2}}(T'_{k+1}-T'_k) + \dot{\sigma}_{k-\frac{1}{2}}(T'_k-T'_{k-1})\right]$$

$$- \frac{1}{2\Delta\sigma_k}\left[(To_{k+1}-To_k)\{\sigma_{k+\frac{1}{2}} . \sum_{j=1}^{N} \Delta\sigma_j . \vec{V}_j . \nabla\ell np_* - \sum_{j=1}^{k} \Delta\sigma_j . \vec{V}_j . \nabla\ell np_*\}\right]$$

$$- \frac{1}{2\Delta\sigma_k}\left[(To_k-To_{k-1})\{\sigma_{k-\frac{1}{2}} . \sum_{j=1}^{N} \Delta\sigma_j . \vec{V}_j . \nabla\ell np_* - \sum_{j=1}^{k-1} \Delta\sigma_j \vec{V}_j . \nabla\ell np_*\}\right]$$

$$-\kappa . To_k \left[\sum_{j=1}^{N} C_{kj}(V_j . \nabla\ell np_*)\right]$$

$$- \kappa Tv'_k \left[\sum_{j=1}^{N} C_{kj} \quad (\vec{V}_j . \nabla\ell np_* + D_j)\right]$$

$$+ \kappa Tv_k . (\vec{V}_k . \nabla\ell np_*)$$

and also

$$T_{v_k} = T_{v_k} - T_k = T'_{v_k} - T'_k$$

$$\mathcal{Q}_k = - \frac{1}{a(1-\mu^2)} \frac{\partial}{\partial\lambda} (U_k . q_k) - \frac{\partial}{a\partial\mu} (V_k . q_k) + D_k . q_k$$

$$- \frac{1}{2\Delta\sigma_k} \left[\dot{\sigma}_{k+\frac{1}{2}} . (q_{k+1} - q_k) + \dot{\sigma}_{k-\frac{1}{2}} . (q_k - q_{k-1}) \right]$$

$$P = - \sum_{j=1}^{N} \Delta\sigma_j . (\vec{V}_j . \nabla \ell n p_*)$$

The elements of matrix $\underline{\tau}$ in the thermodynamic equation are defined as:

$$\tau_{kj} = \frac{1}{2\Delta\sigma_k} \left[(To_{k+1} - To_k) \left\{ \sigma_{k+\frac{1}{2}} . \Delta\sigma_j - \begin{cases} 0 & (k < j) \\ \Delta\sigma_j & (k \geq j) \end{cases} \right\} \right]$$

$$+ \frac{1}{2\Delta\sigma_k} \left[(To_k - To_{k-1}) \left\{ \sigma_{k-\frac{1}{2}} . \Delta\sigma_j - \begin{cases} 0 & (k-1 < j) \\ \Delta\sigma_j & (k-1 \geq j) \end{cases} \right\} \right]$$

$$+ \kappa To_k \, G_{kj}$$

Finally the elements of row vector $\vec{\pi}$ are defined as $\pi_k = \Delta\sigma_k$.

Appendix 2

In this appendix we derive the formula used to compute the r.h.s. of the Helmholtz equation on the gaussian grid.

The solution of the Helmholtz equation (5.11) may be written:

$$\bar{D}^{t}_{m,n\downarrow} = \underline{\underline{A}}_{n}^{-1} \cdot \left[\frac{a^2}{n(n+1)} D^{t-\Delta t}_{m,n\downarrow} + \Delta t . I_{m,n\downarrow} \right]$$

with $$I_{m,n\downarrow} = R_{m,n\downarrow} + \frac{a^2}{n(n+1)} \mathcal{D}_{m,n\downarrow} + \Delta t . R . \underline{\underline{B}} \; T1_{m,n\downarrow}$$

$$R_{m,n\downarrow} = (\phi_{*} + R . \underline{\underline{B}} . T^{t-\Delta t}_{\downarrow} + \Delta t . R \underline{\underline{B}} \; T2_{\downarrow} + RTo_{\downarrow} \ell n p^{t-\Delta t}_{*} + \Delta t \; RT_{o\downarrow} P + R \underline{\underline{B}} \; T_{v\downarrow})_{m,n}$$

T_1 and T_2 have been defined in Appendix 1, the other quantities in Chapter II.

The term $I_{m,n}$ cannot be evaluated in spectral space because two different time levels and tendencies are involved. It is therefore computed on the gaussian grid.

After computation and subsequent Fourier transformation of the terms R, Fu, Fv, UT', VT', E on a gaussian latitude, we have

$$R_{m,n\downarrow} = \sum_{j} w_j \, R^{m}_{\downarrow}(\mu_j) \, P_{m,n}(\mu_j)$$

$$\mathcal{D}_{m,n} = \sum_{j} w_j \left[\left(\frac{im}{a(1-\mu_j^2)} . Fu^{m}_{\downarrow}(\mu_j) + \frac{n(n+1)}{a^2} E^{m}_{\downarrow}(\mu_j) \right) P_{m,n}(\mu_j) - \frac{d}{a d\mu} P_{m,n}(\mu_j) . Fv^{m}_{\downarrow}(\mu_j) \right]$$

$$T1_{m,n} = \sum_{j} w_j \left[\frac{-im}{a(1-\mu_j^2)} (UT')^{m}_{\downarrow} P_{m,n}(\mu_j) + (VT')^{m}_{\downarrow} \frac{d}{a d\mu} P_{m,n}(\mu_j) \right]$$

where upper index m indicates the m-th Fourier component and the vertical arrow a column vector over the vertical levels, as before.

This leads to the following expression for the gaussian contribution of the j-th gaussian latitude to $\Delta t.I_{m,n\downarrow}$

$$\frac{\Delta t}{a(1-\mu_j^2)} \cdot w_j \Big[\{ a(1-\mu_j^2) R^m_{\downarrow}(\mu_j) + \frac{a^2}{n(n+1)} .imFu^m_{\downarrow}(\mu_j) - \Delta t.im.R.\underline{\underline{B}}(UT')^m_{\downarrow} + aE^m_{\downarrow}(\mu_j) \} P_{m,n}(\mu_j)$$

$$- \{ \frac{a^2}{n(n+1)} Fv^m_{\downarrow}(\mu_j) - \Delta t.R.\underline{\underline{B}}(VT')^m_{\downarrow} \} (1-\mu_j^2) \frac{d}{d\mu} P_{m,n}(\mu_j) \Big]$$

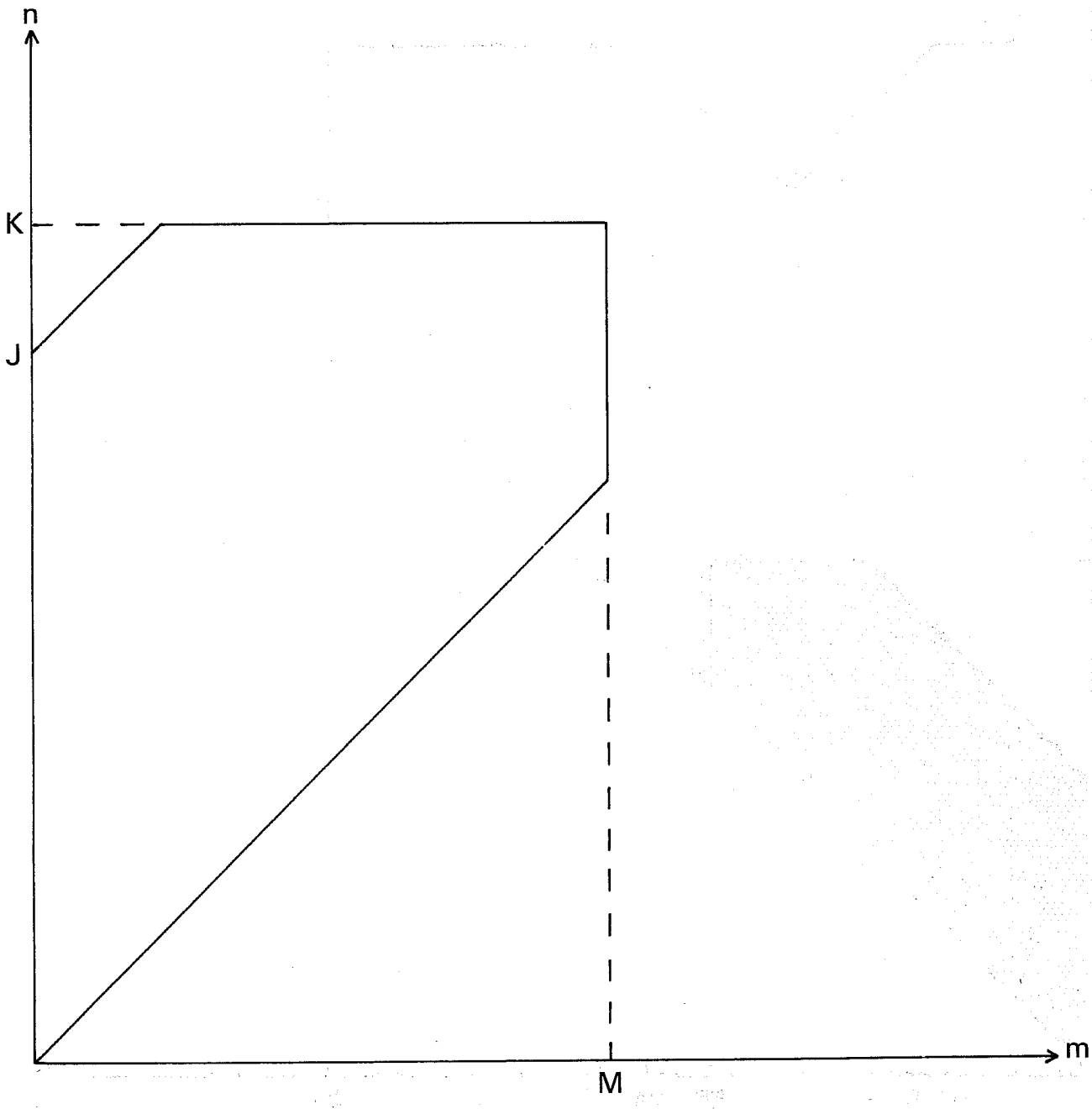

Fig. 2.1 Pentagonal truncation

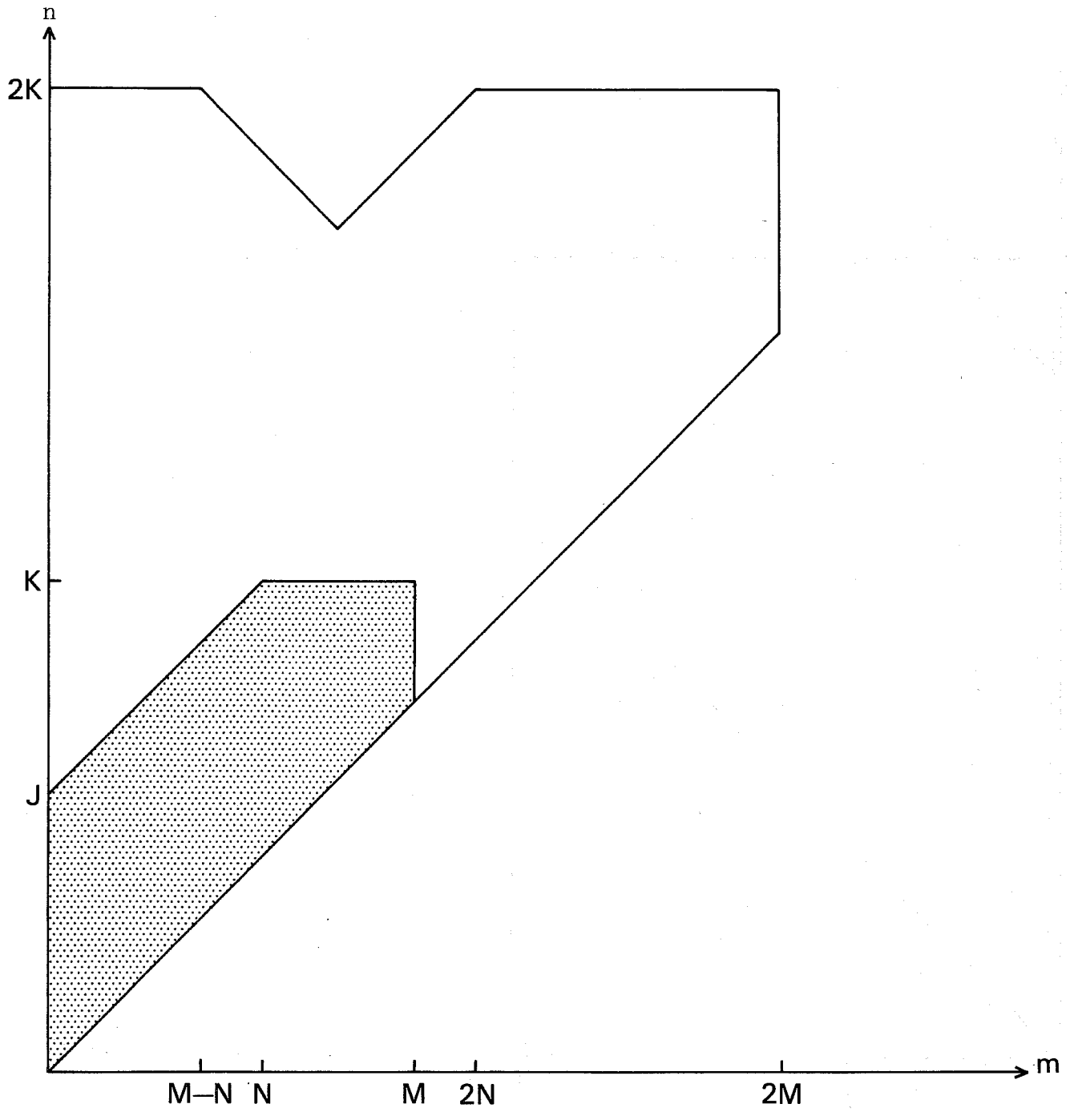

Fig. 2.2 Product truncation

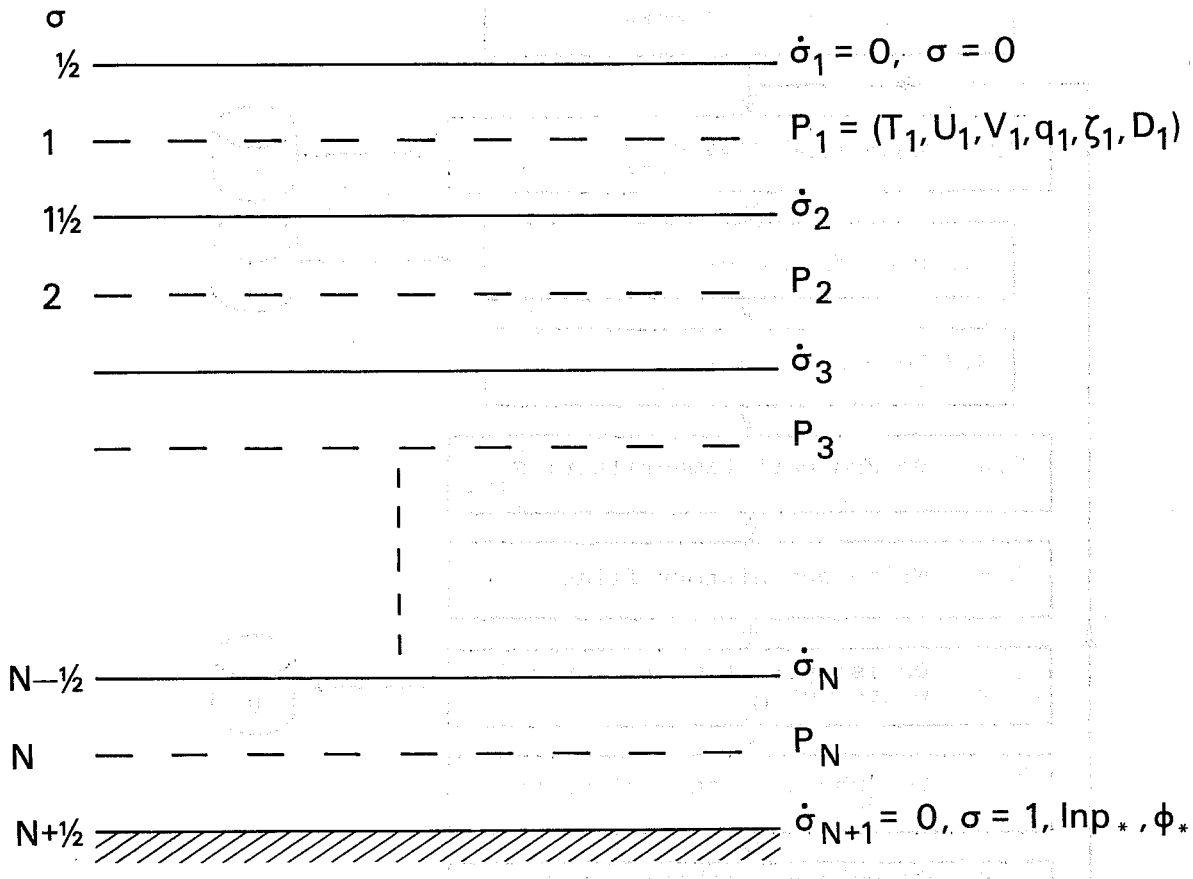

Fig. 3.1 Vertical distribution of variables

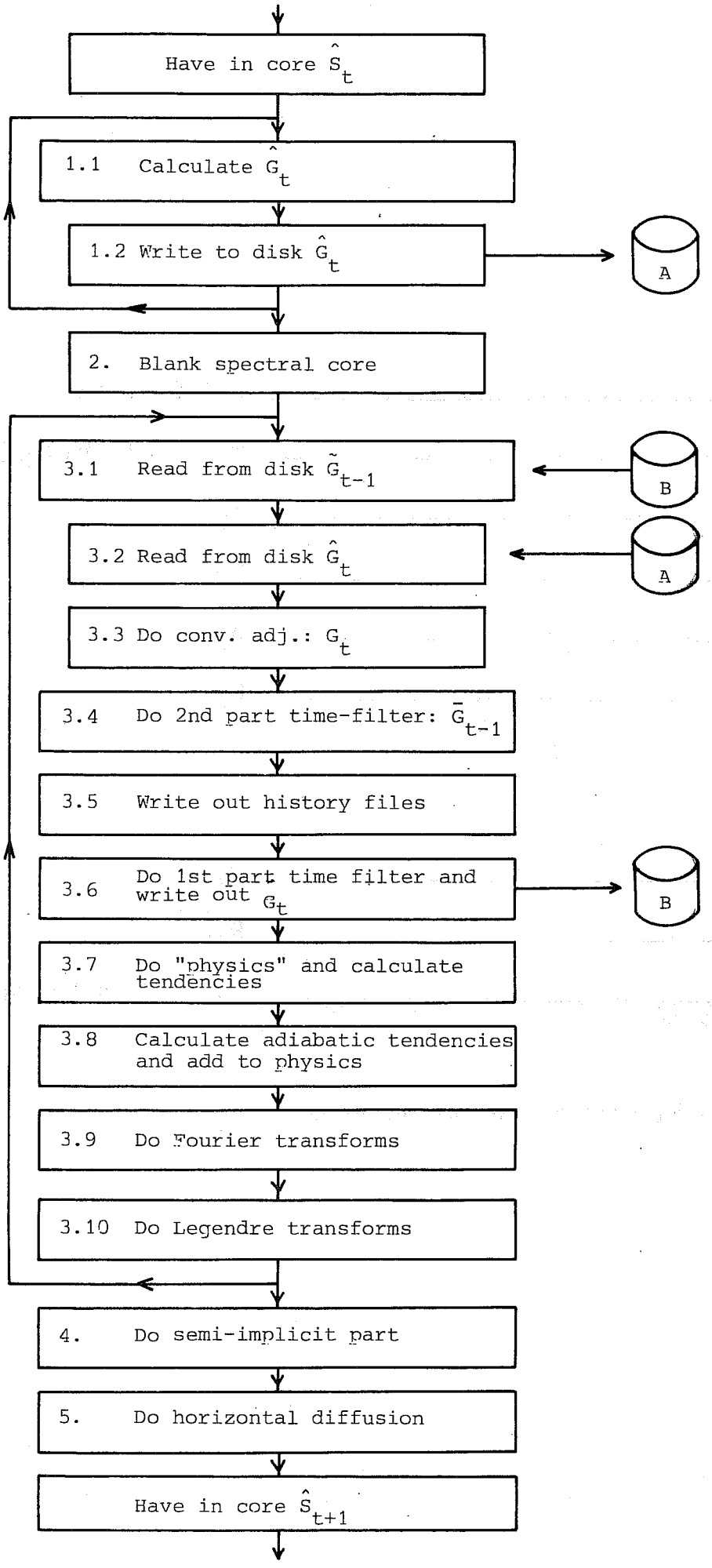

Fig. 10.1 Scheme of double loop time step

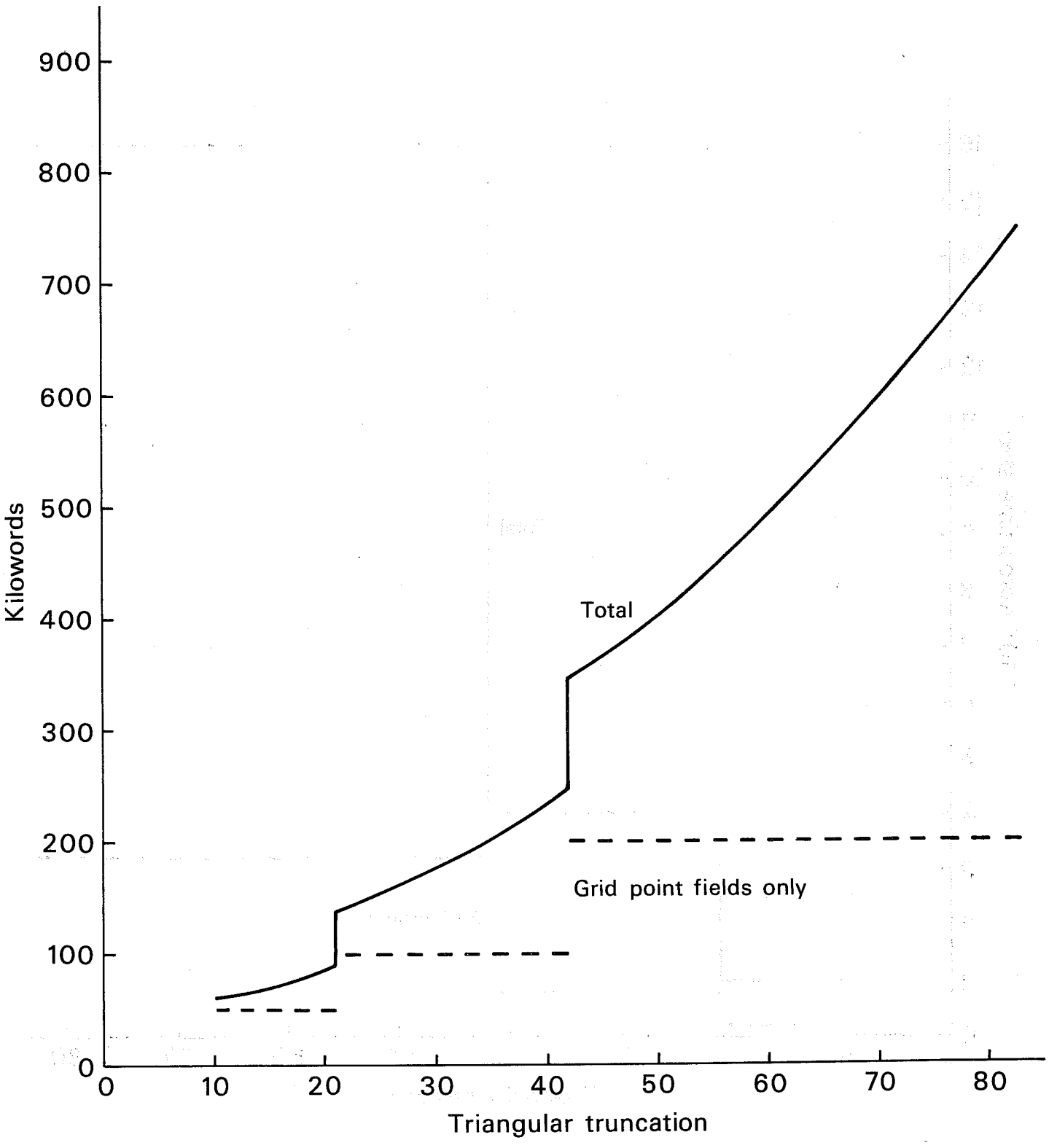

Fig. 10.2 Total memory needed for the spectral and gridpoint fields for a 15 levels adiabatic model. (The number of points on latitude lines is supposed to be a power of 2)

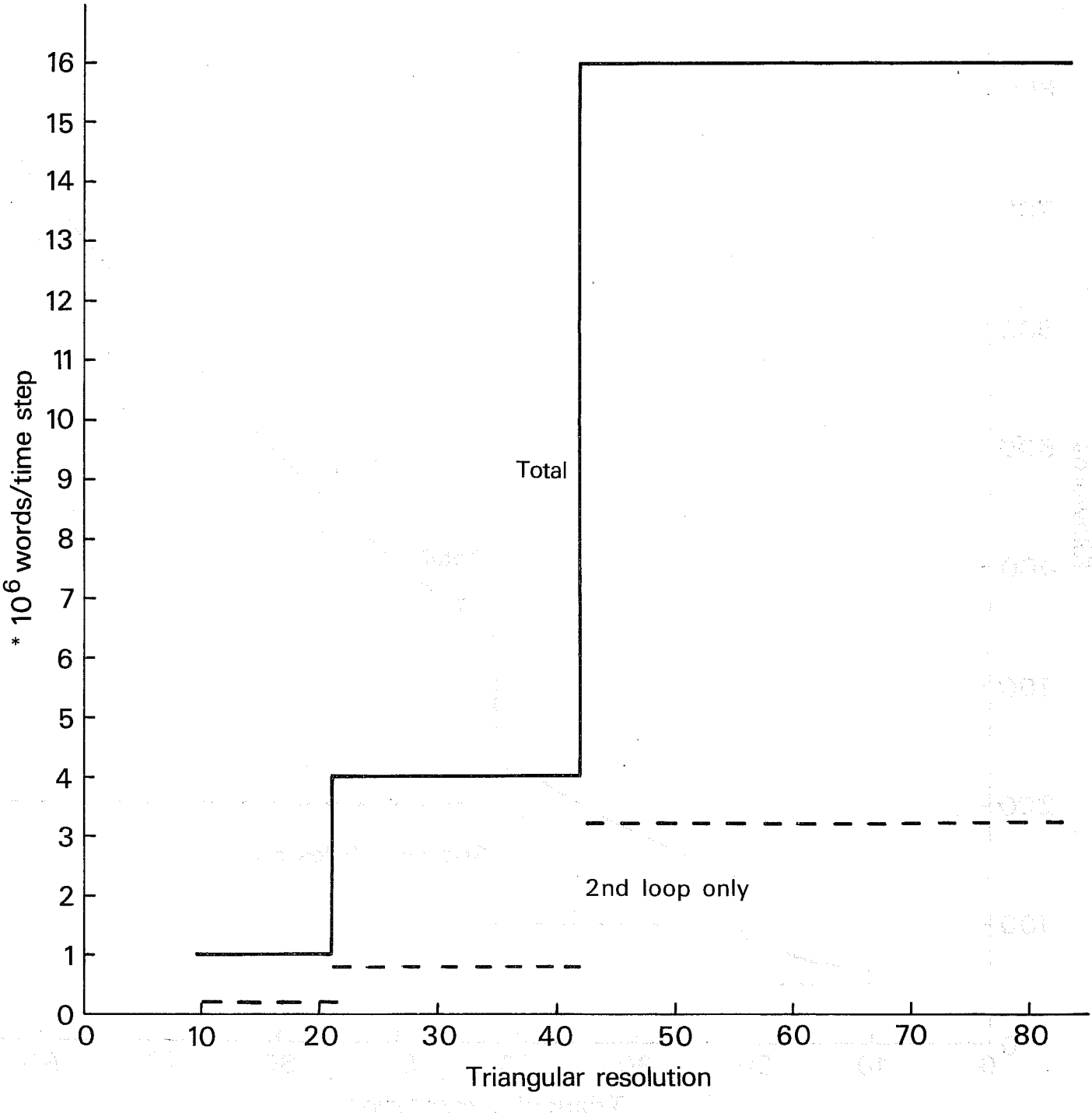

Fig. 10.3 Total I/O per time step

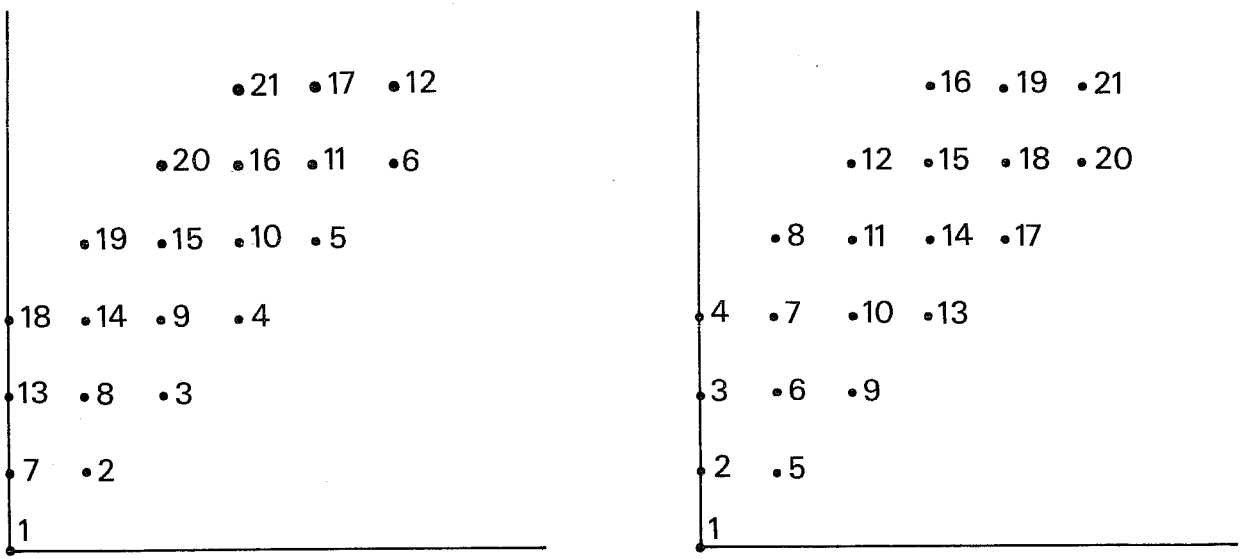

a) diagonal storage

b) column storage

Fig. 11.1 Example of pentagonal truncation

EUROPEAN CENTRE FOR MEDIUM RANGE WEATHER FORECASTS

Technical Report No. 15

No. 1 A Case Study of a Ten Day Prediction

No. 2 The Effect of Arithmetic Precision on some Meteorological Integrations

No. 3 Mixed-Radix Fast Fourier Transforms without Reordering

No. 4 A Model for Medium-Range Weather Forecasting - Adiabatic Formulation -

No. 5 A Study of some Parameterizations of Sub-Grid Processes in a Baroclinic Wave in a Two-Dimensional Model

No. 6 The ECMWF Analysis and Data Assimilation Scheme - Analysis of Mass and Wind Fields

No. 7 A Ten Day High Resolution Non-Adiabatic Spectral Integration : A Comparative Study

No. 8 On the Asymptotic Behaviour of simple Stochastic-Dynamic Systems

No. 9 On Balance Requirements as Initial Conditions

No.10 ECMWF Model - Parameterization of Sub-Grid Scale Processes

No.11 Normal Mode Initialisation for a multi-level Gridpoint Model

No.12 Data Assimilation Experiments

No.13 Comparison of medium range Forecasts made with two Parameterization Schemes

No.14 On Initial Conditions for Non-Hydrostatic Models

No.15 Adiabatic formulation and organisation of ECMWF's spectral model